On the Sensitivity of Ring-Down Observed Inter-Area Modes in Large-Scale Electric Grids Using a Simulation Approach

Wei Trinh, Sanjana Kunkolienkar, Yijing Liu, Thomas J Overbye
Department of Electrical and Computer Engineering
Texas A&M University
College Station, USA
{weit1, sanjanakunkolienkar, yiji21 overbye}@tamu.edu

***Abstract*— This paper presents results on the sensitivity of the inter-area electromechanical modes obtained by ring-down, measurement-based modal analysis for large-scale electric grids. The paper utilizes the Iterative Matrix Pencil Method (IMP) to determine the most significant electro-mechanical modes and their associated mode shapes after the system has been perturbed by generator or load outage contingencies. The paper shows that the resultant values can be dependent on both the applied contingency and the set of signals used in the IMP with this sensitivity due at least in part to the system nonlinearities. The techniques are demonstrated using three synthetic grids ranging in size between 2000 and 70,000 buses. Visualization methods are used to show the mode shapes and compare and contrast how modes manifest themselves on the grid.**

I. Introduction

Electric grids oscillate, with the study of these oscillations an area of interest for many decades [1], [2]. Initially the oscillations were mostly associated with individual generators, but as system began to interconnect over larger distances the concept of inter-area (or wide-area) oscillations arose, with [3] providing a nice coverage of the oscillations in the North American Western Grid (now known as the WECC) when it first interconnected in 1964. A nice coverage of the fundamentals of power system oscillations is given in [4].

Over the years several techniques for analyzing these oscillations have developed, with the analog technique of [3] (in which the oscillations were expressed in integer cycles per minute) giving way as digital computers developed to eigenvalue analysis [5], [6] in which detailed system models are used with the system linearized about an operating point. Assuming such a linearized model is valid, the eigenvalues then give the frequency and damping of the different modes, and the associated right eigenvector then tells how the different electric grid devices such as generators participate in the mode; further details on specific of eigenvalue analysis are given in [7] and [8].

More recently there has been increased application of signal-based modal analysis techniques, with a number of different methods available. These methods are divided into two main classes: ring-down and the ambient data. In the ring-down approach, which is the focus of this paper, a disturbance (contingency) occurs on the electric grid and then the algorithm tries to reproduce one or more of the associated signals using a set of basis functions, with the basis functions usually a set of exponentially scaled sinusoidals. Common methods include Prony [9], Matrix Pencil [10], Variable Projection Method [11], Dynamic Model Decomposition [12], and the Iterative Matrix Pencil (IMP) [13]. The obtained exponential functions are then used to define the modes. The second approach utilizes ambient data, in which the continuous small fluctuations that are always occurring on the electric grid are used to determine the observed modes. Examples of this approach are given in [14], [15], [16].

The purpose of this paper is to assess the sensitivity of the electromechanical modes observed using the ring-down approach to both the location of the contingency and the set of signals used to determine the modes. The motivation for this work is to consider the degree to which an analysis technique developed for linear systems can be used on large-scale electric grids.

Measurement-based modal analysis can be done either using results from actual electric grids, usually with the input signals coming from phasor measurement units (PMUs), or from electric grid simulations. While works focused on actual data can certainly be beneficial, in the context of this paper simulation results provide the following advantages. First, results can be provided for both models of actual grids and for synthetic electric grids [17] with a key advantage of synthetic grids being that full results can be provided since they do not have restricted availability (e.g., in the US some information about electric grids is considered to be critical energy/electricity infrastructure information (CEII) that cannot be publicly disclosed [18]). Second, arbitrary contingencies can be simulated, which will be crucial for determining the sensitivities of the modes to the disturbance location. Third, all signals are available, allowing for assessing the sensitivities of the calculated modes to the input signals.

The remainder of the paper is organized as follows. The next section presents the test grids. The third section then discusses the study procedure, followed by a section containing results. The last section summarizes the paper and presents directions for future work. All calculations and visualizations were done using PowerWorld Simulator.

II. Test Grids

Given the focus of the paper on large-scale electric grids, the three grids considered here have at least several thousand buses. In addition they are synthetic, with the details on the development and validation of these grids given in [17], [19], [20], [21]; all three are assumed to have a nominal frequency of 60 Hz. The first is a 2000-bus (2K), 544-generator, 67 GW load grid covering much of the US state of Texas with the grid oneline shown in Figure 1. The second is a 10,000-bus, 2500-generator, 151 GW load grid covering the US portion of the WECC with its oneline shown in Figure 2, while the third is a 70,000-bus (70K), 10,400-generator, 600 GW grid covering the eastern part of the US (Figure 3). In the figures the different line colors are used to indicate the line's nominal voltage with green for 765kV, orange for 500 kV, red for 345 kV, purple for 230 kV and black for the lower voltage levels. In general all three synthetic grids were designed to use nominal voltages not used in the actual grids, all have substations with geographic coordinates, and all are available for download at [22].

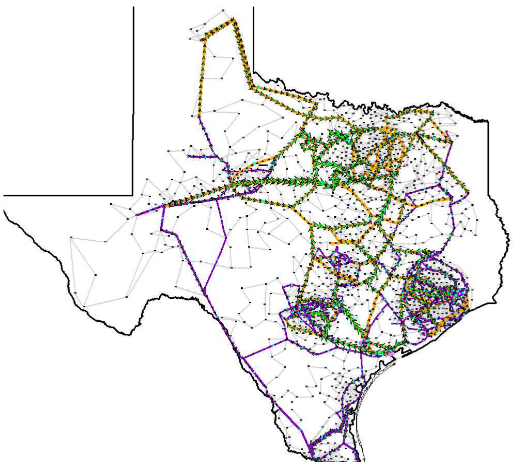

Figure 1: 2K Grid Synthetic Grid Oneline

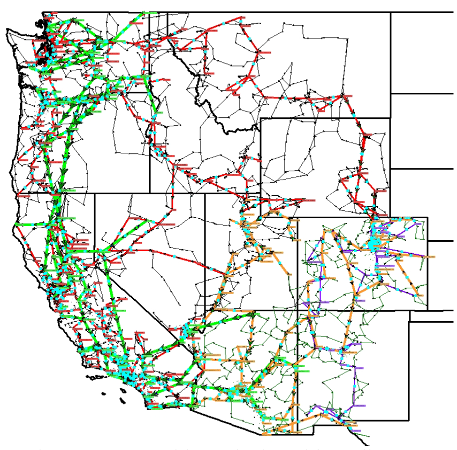

Figure 2: 10K Grid Synthetic Grid Oneline

All the grids have standard transient stability-level dynamic models, including models for the machines, the exciters, the governors and the stabilizers. By far the most complex in terms of models is the 70K grid, which has 19 different model classes, 40,400 model instances, and when solved 191,700 state variables. Hence its linearized response would have a large number of modes, though most are associated with the individual generators, with significantly fewer inter-area, electromechanical modes. Of note is some of the model instances have quite nonlinear behavior, including deadbands, state variables at limits, and an asymmetric response for some, such as governor whose output is not allowed to move up. A focus of this paper is to determine how much these nonlinearities affect the mode modeling approximations.

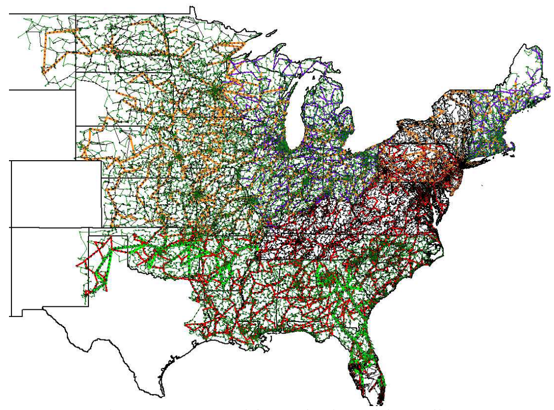

Figure 3: 70K Grid Synthetic Grid Oneline

III. Procedure

The general procedure to assess the sensitivity of the ring-down observed inter-area modes is to first, for each test grid, simulate the response of the grid to a variety of different contingencies, storing the frequency signals for each bus for each contingency. These signals then provide the inputs for the subsequent ring-down analysis. For these signals the Iterative Matrix Pencil method (IMP) [13] is then used to calculate the observed modes. Also, the computation insight from [11] is used to determine how each signal participates in each mode. Because of the high correlation of many of the bus frequency signals, an insight utilized in the IMP is that only of small number of signals (usually no more than ten) is needed to calculate all the significant electromechanical inter-area modes for even a large system. The results can then be visualized, leveraging recent techniques such as those from [23], [24].

This procedure can be illustrated using two contingencies on the 2K grid, with the first contingency the loss of the 1196 MW generator at bus 5262, and the second loss of the 1350 MW generator at bus 7099. In both contingencies the generator loss occurs at simulation time of 1.0 second, and the simulation runs for a total of 20 seconds; the solution is done using a time step of 0.5 cycles. The frequency signals for all 2000 buses are shown respectively for the two contingencies in Figure 4 and Figure 5. This data is then the inputs utilized in the subsequent comparisons.

The next step is to utilize the IMP to calculate the observed modes utilizing all 2000 bus frequency signals. The calculated sinusoidal modes for each contingency are shown, respectively, in Table 1 and Table 2 with the first column giving the frequency of the mode, the second its damping [7], the third the largest component of the mode in a signal, the fourth the average component in all the signals, and the last the bus number of the location with the highest component value.

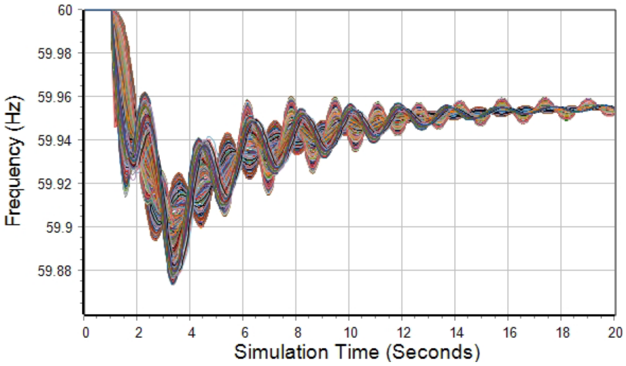

Figure 4: 2K Grid Bus Frequencies for Bus 5262 Gen Open Contingency

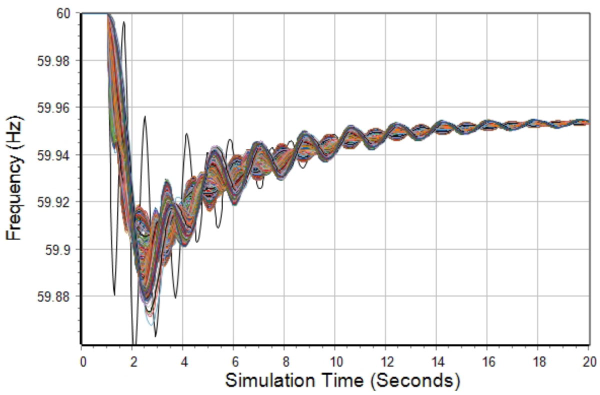

Figure 5: 2K Grid Bus Frequencies for Bus 7099 Gen Open Contingency

Table 1: Main Electromechanical Modes for Bus 5262 Gen Contingency

Freq (Hz)	Damping (%)	Largest Value (Hz)	Average Value (Hz)	Bus of Largest
0.191	66.82	0.3012	0.1450	1073
0.531	5.75	0.0526	0.031	2120
0.625	2.87	0.0326	0.0053	4192
0.886	10.07	0.0122	0.003	1051
1.531	8.44	0.0113	0.0011	3056
0.042	-13.56	0.003	0.0026	2057

Table 2: Main Electromechanical Modes for Bus 7099 Gen Contingency

Freq (Hz)	Damping (%)	Largest Value (Hz)	Average Value (Hz)	Bus of Largest
0.190	60.76	0.2037	0.094	1073
1.205	5.62	0.0930	0.0031	7098
1.45	27.75	0.0372	0.0075	1073
0.552	3.96	0.0260	0.0151	2120
0.934	5.73	0.0211	0.0060	6147
0.027	-6.35	0.0098	0.0084	7098
0.614	4.085	0.00561	0.00176	4192

The heart of the paper is then a discussion of how the associated contingencies, the set of frequency signals used in the IMP, system non-linearities, and the system size impact the results. Mode shape visualization techniques from [23] are used to show the sensitivity of the mode shapes. Examples of such visualizations are shown in Figures 6 to 9, with Figures 6 and 7 showing that the mode at about 0.54 Hz is very similar between the contingencies, whereas the 0.625 Hz mode is quite different (in the figures the arrows show the magnitude of the mode shape at different locations in the grid, whereas the arrow direction shows the phase relationships; a consistent arrow scaling is used between the figures to aid in comparisons). In order to quantify the differences between the different manifestations of modes, the mode shapes are normalized, and the dot product between the two different sets of mode shapes is taken. This value ranges from -1 to 1, indicating whether or not the mode shape angles are in phase or out of phase with each other, with 1 being in phase, and -1 being 180 degrees out of phase. Due to the size of these systems, contours serve as a useful visualization technique that is used in conjunction with the quantification of the mode shapes [25].

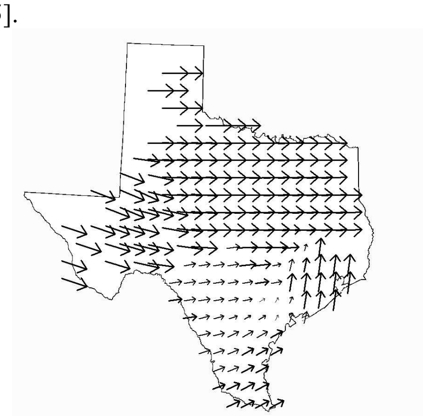
Figure 6: 0.531 Hz Mode Shape for 2K 5262 Gen Contingency

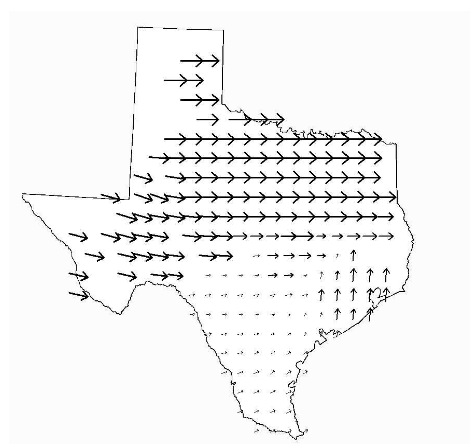
Figure 7: 0.552 Hz Mode Shape for 2K 7099 Gen Contingency

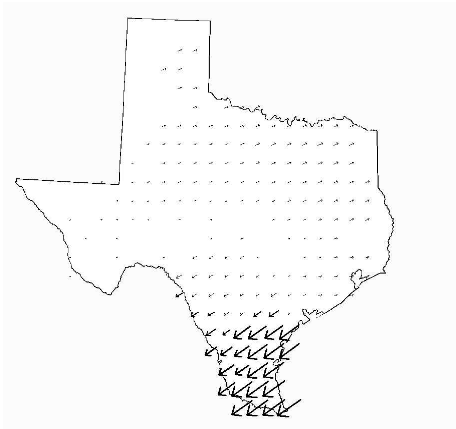

Figure 8: 0.625 Hz Mode Shape for 2K 5262 Gen Contingency

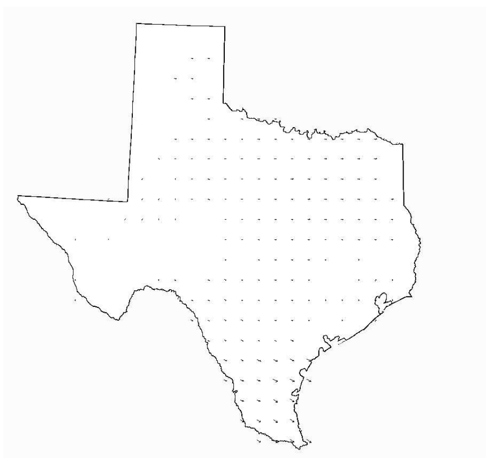

Figure 9: 0.614 Hz Mode Shape for 2K 7099 Gen Contingency

IV. RESULTS

For the 10,000-bus system, which is a synthetic gird covering the Western United States, several contingencies are chosen. These contingencies each involve one generator being taken out of service, with the generator size being one of the largest ones in the grid. The three largest generators taken out of service individually are the ones with generation capacity of 1403 MW at bus 40844, 1161 MW at bus 26133 and 1082 MW at bus 11019. The bus 40844 is located in Arizona; bus 26133 is located in south-west California and bus 11019 is located in Washington. These three contingencies produced about 10 modes on average, using the IMP method, with the four most similar mode frequencies listed in Table 3 along with the corresponding damping percentages in Table 4.

Table 3: Similar Mode Frequencies between Contingencies for 10k Bus System

	40844 Bus Mode Frequency (Hz)	26133 Bus Mode Frequency (Hz)	11019 Bus Mode Frequency (Hz)
Mode 1	0.690	0.687	0.706
Mode 2	0.613	0.612	0.646
Mode 3	0.474	0.473	0.479
Mode 4	0.379	0.374	0.390

Table 4: Dampings for Modes between Contingencies for 10k Bus System

	40844 Bus Mode Damping (%)	26133 Bus Mode Damping (%)	11019 Bus Mode Damping (%)
Mode 1	3.224	5.002	2.736
Mode 2	5.106	5.691	5.501
Mode 3	7.221	7.050	5.889
Mode 4	9.355	10.285	9.280

The frequency response for the contingency at bus 11019 is seen in Figure 10. Figures 11 to 13 show how mode 1 from all three contingency cases manifests itself on the grid. The mode 1, despite being close in frequency and magnitude across contingencies, a preliminary visual inspection shows that it manifests differently. In line with the observation in 2k bus case, the modes do not manifest consistently across the grid even for the 10k bus case. From Figures 11-13 it is clear that the direction of mode is similar in California, east Montana, east Wyoming and Arizona for the generator contingency at bus 40844 and bus 26133. The direction of mode magnitude is opposite in the same locations for the generator contingency at bus 11019.

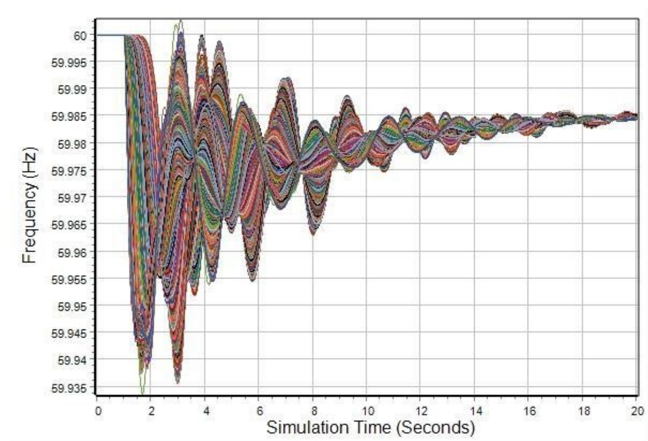

Figure 10: 10k Grid Bus Frequencies for Bus 11019 Gen Open Contingency

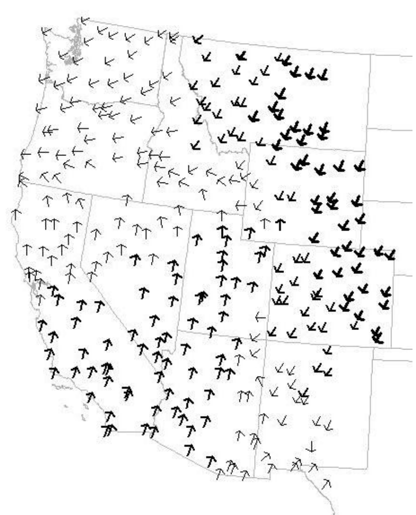

Figure 11: 0.474 Hz Mode Shape for 10K 40844 Gen Contingency

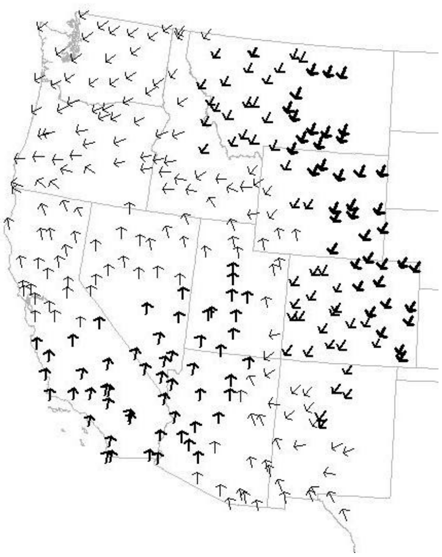

Figure 12: 0.473 Hz Mode Shape for 10K 26133 Gen Contingency

Alternatively, for mode four from Table 5, the manifestation of both magnitude and direction is quite different for the generator contingency at bus 40844 (0.379 Hz) and bus 26133 (0.373 Hz), as observed in Figures 14 and 15.

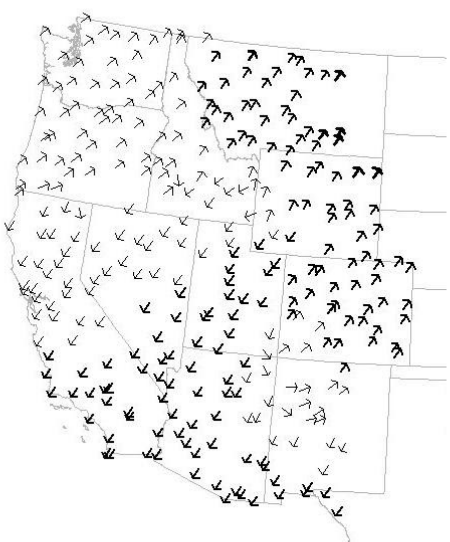

Figure 13: 0.479 Hz Mode Shape for 10K 11019 Gen Contingency

Quantifying these results through the dot product of the normalized mode shapes, we arrive at Figures 16 and 17. The stark difference between the two figures further emphasizes that while this mode can express itself consistently between contingencies, it is not guaranteed to maintain that behavior when considering multiple different types of contingencies which produce modes at the same frequency.

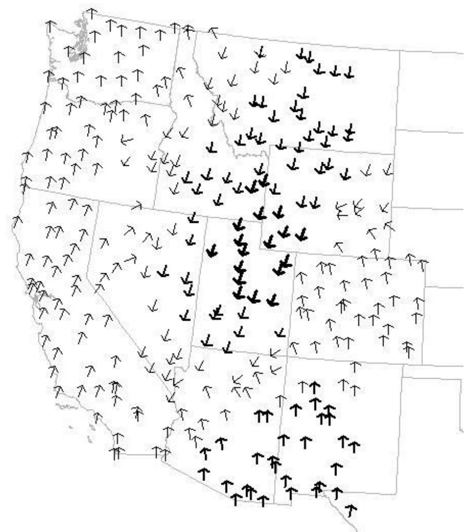

Figure 14: 0.379 Hz Mode Shape for 10K 40844 Gen Contingency

The methodology is then extended to a 70,000-bus synthetic network, which encompasses the footprint of the Eastern United States interconnect. The three contingencies of interest will be the separate outage of two of the largest generators of the system, located at Buses 30902 and 38341, and an outage of similar magnitude at Bus 28344, geographically located in southern Florida. An example of the frequency response to each of these contingencies is seen in Figure 18, where several stabilizers from the system have been removed.

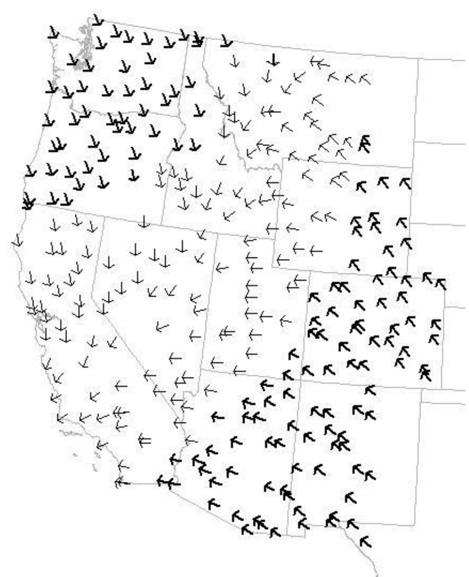

Figure 15: 0.373 Hz Mode Shape for 10K 26133 Gen Contingency

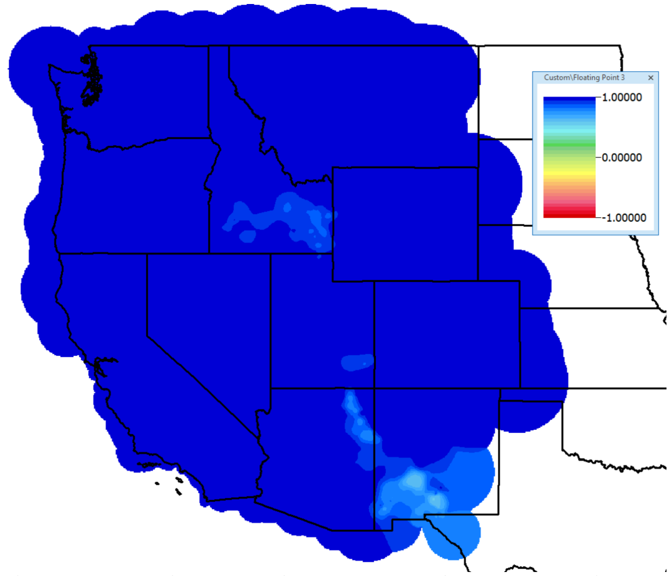

Figure 16: Dot Product Contour between 40844 and 26133 Gen Contingency

For the contingency that involved the generator at Bus 28344 opening, 13 modes were observed using the IMP method, ranging from 0.02 Hz to 2.74 Hz. For the contingency that involved the generator at Bus 30902 being opened, 13 modes were observed ranging from 0.03 Hz to 1.491 Hz. Finally, for the contingency where the generator at Bus 38341 was opened, 21 modes were observed, with a minimum frequency of 0.021 Hz and a maximum of 4.362 Hz.

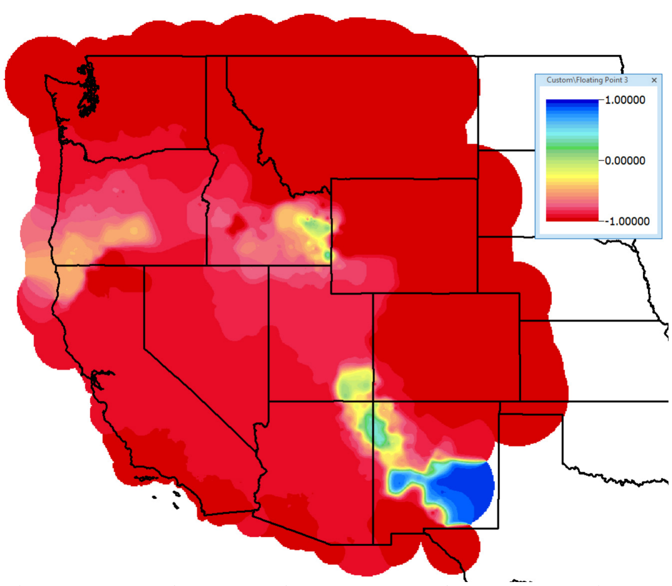

Figure 17: Dot Product Contour between 40844 and 11019 Gen Contingency

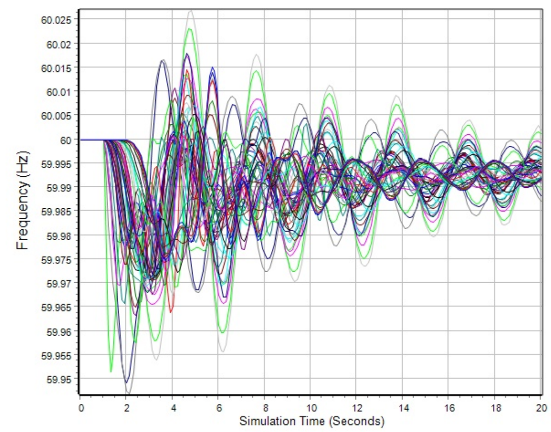

Figure 18: 70k Grid Average Bus Frequencies for Bus 30902 Gen Open Contingency

The first objective is to take the resulting modes and identify similar frequency modes between each of the contingencies. For the three contingencies selected, the similar modes are observed in Table 5. The dampings are presented in Table 6. It is apparent that for such a large system, unlike the 2000 bus system, there is a higher variance in the number of modes produced by the IMP method. Given these results, the next step is to visualize how the modes manifest themselves in the system via their mode shapes.

Table 5: Similar Mode Frequencies between Contingencies for 70k Bus System

	28344 Bus Mode Frequency (Hz)	30902 Bus Mode Frequency (Hz)	38341 Bus Mode Frequency (Hz)
Mode 1	0.264	0.243	0.209
Mode 2	0.324	0.329	0.316
Mode 3	0.578	0.573	0.577
Mode 4	0.698	0.679	0.699

Table 6: Dampings for Modes between Contingencies for 70k Bus System

	28344 Bus Mode Damping (%)	30902 Bus Mode Damping (%)	38341 Bus Mode Damping (%)
Mode 1	37.406	28.407	38.708
Mode 2	4.19	3.987	4.459
Mode 3	6.912	6.589	5.847
Mode 4	3.515	5.052	4.257

Figures 19 to 21 show how the one of the modes that the contingencies share manifests itself on the grid. By observation, it is clear that despite being similar in frequency and damping, the modes do not manifest themselves consistently across the grid. While certain areas of the grid are similar in nature, there is no significant geographical location in the grid whose mode shapes are consistent in both magnitude and phase between all three contingencies.

Figure 19: 0.264 Hz mode Shape for 70k 28344 Gen Contingency

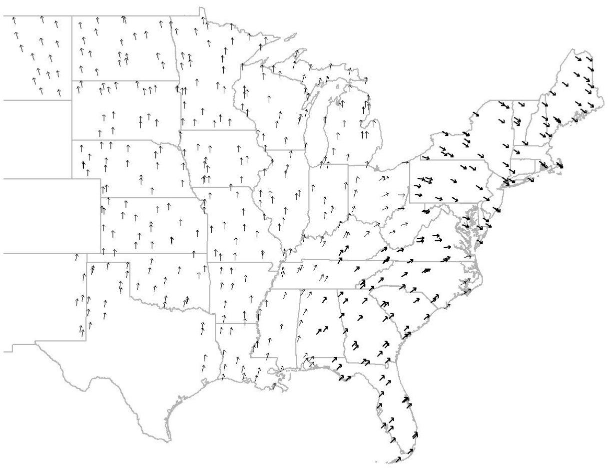

Figure 20: 0.243 Hz Mode Shape for 70K 30902 Gen Contingency

Figure 21: 0.209 Hz Mode Shape for 70K 38341 Gen Contingency

Even more striking are the differences expressed in the northwestern part of the grid, where the mode shapes point in completely different directions between contingencies. Using the quantitative approach described in Section III, contours of the Euclidean distance for each bus in the system can be seen in Figures 22 and 23.

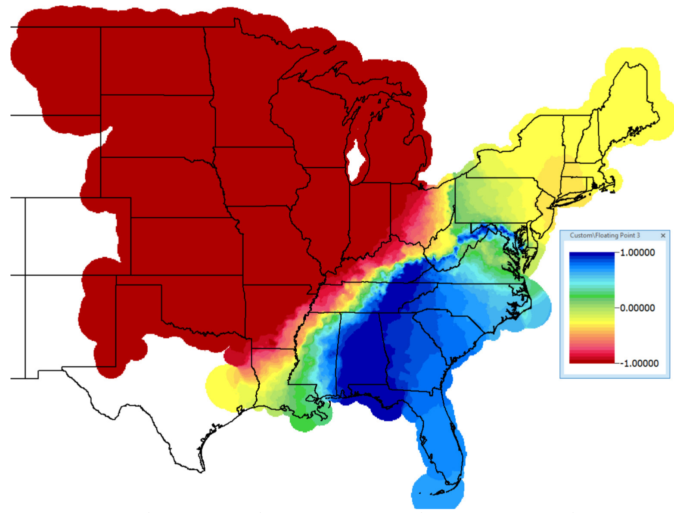

Figure 22: Dot Product Contour between 30902 and 28344 Gen Contingency

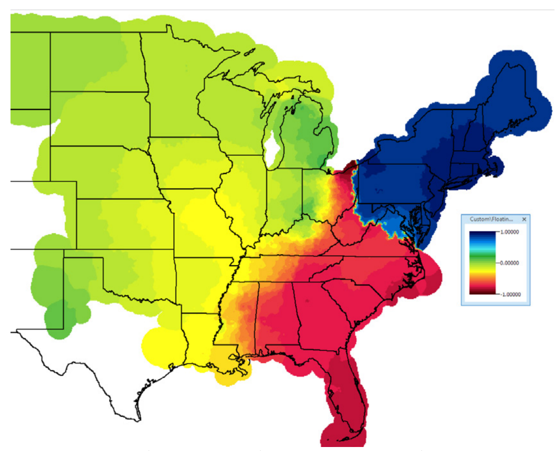

Figure 23: Dot Product Contour between 30902 and 38341 Gen Contingency

Through observation of the contours, we see that while there are areas where the mode shapes are similar across regions, there are also pockets of much larger differences. This is especially emphasized when looking at different contingencies, where two contingencies may potentially share somewhat similar mode manifestation, but when contrasted against other contingencies with modes at similar frequencies, the manifestations are significantly more deviated. The implications of such results indicates that the modes that are of similar frequency may be entirely different modes, which have differing weights and impacts on the bus frequency data depending on what type of contingency is considered, along with where the contingency is located.

V. Summary And Future Directions

This paper has addressed the question of how modes may change depending on the contingency and signals that are considered when calculating the modes. In particular, this paper displays that despite similar frequencies and dampings, depending on the contingencies, modes may manifest themselves in vastly different ways through their mode shapes. This notion brings about future work, discussing the origin of modes, and what conditions are necessary for a mode to exist.

VI. Acknowledgments

This work was partially supported through funding provided by the U.S. National Science Foundation in Award 1916142, the US ARPA-E, and the Power Systems Engineering Research Center (PSERC).

References

[1] C. Concordia, S. B. Crary, J.M. Lyons, Stability Characteristics of Turbine Generators, AIEE Transactions, vol. 57, pp. 732-744, 1938.

[2] C. Concordia, G. Kron, *AIEE Transactions*, "Damping and Synchronizing Torques in Power Systems," vol. 64, pp. 366-371, 1945

[3] F.R. Schleif, J.H. White, "Damping for the Northwest – Southwest Tieline Oscillations – An Analog Study," *IEEE Trans. Power App. & Syst*., vol. PAS-85, pp. 1239-1247, December 1966.

[4] M. Klein, G.J. Rogers, P. Kundur, "A Fundamental Study of Inter-area Oscillations in Power Systems," *IEEE Trans. Power Systems*, vol. 6, pp. 914-921, August 1991.

[5] R.T. Byerly, R.J Bennon, D.E. Sherman, "Eigenvalue Analysis of Synchronizing Power Flow Oscillations in Large Electric Power Systems, *IEEE Trans. Power App. & Syst*., vol. PAS-101, pp. 235-243, January 1982.

[6] P. Kundur, G.J. Rogers, D.Y. Wong, L. Wang, M.G. Lauby, "A Comprehensive Computer Program Package for Small Signal Stability Analysis of Power Systems," *IEEE Trans. Power Sys.*, vol. 5, pp. 1076-1083, November 1990.

[7] P. Kundur, *Power System Stability and Control*, McGraw-Hill, Inc., New York, NY, 1994.

[8] P.W. Sauer, M.A. Pai, J.H. Chow, *Power System Dynamics and Stability*, 2nd Edition, John Wiley & Sons, Ltd, 2018.

[9] J.F. Hauer, C.J. Demeure, and L.L. Scharf, "Initial Results in Prony Analysis of Power System Response Signals," *IEEE Trans. on Power Systems* , vol. 5, no. 1, pp. 80-89, February 1990.

[10] M.L. Crow and A. Singh, "The Matrix Pencil for Power System Modal Extraction," *IEEE Trans. on Power Systems*, vol. 20, no. l, pp. 501-502, February 2005.

[11] A.R. Borden, B.C. Lesieutre, J. Gronquist, "Power System Model Analysis Tool Developed for Industry Use," Proc. 2013 North American Power Symposium, Sept. 2013.

[12] E. Barocio, B. Pal, N. Thornhill, and A. Messina, "A Dynamic Mode Decomposition Framework for Global Power System Oscillation Analysis," *IEEE Trans. Power Systems*, vol. 30, pp. 2902-2912, November 2015.

[13] W.C. Trinh, K.S. Shetye, I. Idehen, T.J. Overbye, "Iterative Matrix Pencil Method for Power System Modal Analysis," 52nd Hawaii International Conference on System Sciences, Waikoloa, HI, Jan 2019.

[14] J.W. Pierre, D.J. Trudnowski, and M. K. Donnelly, "Initial Results in Electromechanical Mode Identification from Ambient Data," *IEEE Trans. Power Syst*., vol. 12, pp. 1245–1251, August 1997.

[15] S.A. Nezam Sarmadi, V. Venkatasubramanian, "Electromechanical Mode Estimation using Recursive Adaptive Stochastic Subspace Identification," *IEEE Trans. Power Syst*., vol. 29, pp. 349–358, Jan 2014.

[16] D. Pandit, D. Pandit, N. Nguyen, S. Elsaiah, "Power System Electrocmechanical Mode Estimation using Lower-Order Recursive Subspace Method," Proc. 53rd North American Power Symposium, College Station, TX, November 2021.

[17] A.B. Birchfield, T. Xu, K. Gegner, K.S. Shetye, T.J. Overbye, "Grid Structural Characteristics as Validation Criteria for Synthetic Networks," *IEEE Trans. Power Syst.*, vol. 32, pp. 3258-3265, July 2017.

[18] Critical Energy/Electric Infrastructure Information, US Federal Energy Regulatory Commission (FERC); available online at www.ferc.gov/ceii .

[19] A.B. Birchfield, E. Schweitzer, M. H. Athari, T. Xu, T.J. Overbye, A. Scaglione, Z. Wang, "A Metric-Based Validation Process to Assess the Realism of Synthetic Power Grids," *Energies*, August 2017.

[20] T. Xu, A.B. Birchfield, K.S. Shetye, T.J. Overbye, "Creation of Synthetic Electric Grid Models for Transient Stability Studies," Proc. 10th Bulk Power Systems Dynamics and Control Symposium (IREP 2017), Espinho, Portugal, Sept. 2017.

[21] T. Xu, A.B. Birchfield, T.J. Overbye, "Modeling, Tuning and Validating System Dynamics in Synthetic Electric Grids," *IEEE Trans. Power Syst.*, vol. 33, pp. 6501-6509, November 2018.

[22] Texas A&M Electric Grid Test Case Repository, https://electricgrids.engr.tamu.edu/.

[23] I. Idehen, B. Wang, K.S. Shetye, T.J Overbye, J.D. Weber, "Visualization of Large-Scale Electric Grid Oscillation Modes," Proc. 50th North American Power Symposium, Fargo, ND, September 2018.

[24] T.J. Overbye, K.S. Shetye, J. Wert, W. Trinh, A. Birchfield, T. Rolstad, J.D. Weber, "Techniques for Maintaining Situational Awareness During Large-Scale Electric Grid Simulations," Proc. 2021 Power and Energy Conference at Illinois, Champaign, IL, April 2021.

[25] J. D. Weber and T. J. Overbye, "Voltage contours for power system visualization," *IEEE Trans. on Power Systems*, pp. 404-409, February, 2000.